Available online at www.sciencedirect.com
SCIENCE DIRECT
Journal of Magnetic Resonance 180 (2006) 147–161
JMR Journal of Magnetic Resonance
www.elsevier.com/locate/jmr

Magnetization-recovery experiments for static and MAS-NMR of $I = 3/2$ nuclei

James P. Yesinowski *

Chemistry Division, Naval Research Laboratory, Washington, DC 20375, USA

Received 30 November 2005; revised 25 January 2006
Available online 21 February 2006

Abstract

Multifrequency pulsed NMR experiments on quadrupole-perturbed $I = 3/2$ spins in single crystals are shown to be useful for measuring spin–lattice relaxation parameters even for a mixture of quadrupolar plus magnetic relaxation mechanisms. Such measurements can then be related to other MAS-NMR experiments on powders. This strategy is demonstrated by studies of ^{71}Ga and ^{69}Ga (both $I = 3/2$) spin–lattice relaxation behavior in a single-crystal (film) sample of gallium nitride, GaN, at various orientations of the axially symmetric nuclear quadrupole coupling tensor. Observation of apparent single-exponential relaxation behavior in $I = 3/2$ saturation-recovery experiments can be misleading when individual contributing rate processes are neglected in the interpretation. The quadrupolar mechanism (dominant in this study) has both a single-quantum process (T_{1Q1}) and a double-quantum process (T_{1Q2}), whose time constants are not necessarily equal. Magnetic relaxation (in this study most likely arising from hyperfine couplings to unpaired delocalized electron spins in the conduction band) also contributes to a single-quantum process (T_{1M}). A strategy of multifrequency irradiation with observation of satellite and/or central transitions, incorporating different initial conditions for the level populations, provides a means of obtaining these three relaxation time constants from single-crystal ^{71}Ga data alone. The ^{69}Ga results provide a further check of internal consistency, since magnetic and quadrupolar contributions to its relaxation scale in opposite directions compared to ^{71}Ga. For both perpendicular and parallel quadrupole coupling tensor symmetry axis orientations small but significant differences between T_{1Q1} and T_{1Q2} were measured, whereas for a tensor symmetry axis oriented at the magic-angle (54.74°) the values were essentially equal. Magic-angle spinning introduces a number of complications into the measurement and interpretation of the spin–lattice relaxation. Comparison of ^{71}Ga and ^{69}Ga MAS-NMR saturation-recovery curves with both central and satellite transitions completely saturated by a train of 90° pulses incommensurate with the rotor period provides the simplest means of assessing the contribution from magnetic relaxation, and yields results for the quadrupolar mechanism contribution that are consistent with those obtained from the film sample.
Published by Elsevier Inc.

Keywords: Quadrupolar NMR; Spin–lattice relaxation; Magic-angle spinning; Single crystal; Gallium nitride

1. Introduction

The magnetization-recovery behavior of quadrupolar nuclei having half-integral spin quantum numbers ($I = 3/2$, 5/2, 7/2, and 9/2) can provide information about dynamical processes, as well as the interactions of these nuclei with conduction electrons in metals and semiconductors, or with localized paramagnetic sites. The description of spin–lattice relaxation in multilevel systems of half-integral quadrupolar nuclei dates back a half century to Pound's original work [1]. Subsequent studies have emphasized solutions to the set of coupled rate equations describing the populations of each level [2–6]. These solutions depend upon both the initial state of the spin system in a given T_1 experiment, as well as the nature of the relaxation mechanism (viz., whether quadrupolar or magnetic in nature). Spin–lattice relaxation via the nuclear magnetic dipole is characterized by a *single* rate process having a rate $W = 1/(2T_{1M})$, which can nevertheless lead to multiexponential relaxation behavior depending upon the initial conditions of the experiment. Relaxation via the

* Fax: +1 202 767 0594.
E-mail address: yesinowski@nrl.navy.mil.

1090-7807/$ - see front matter Published by Elsevier Inc.
doi:10.1016/j.jmr.2006.02.004

nuclear electric quadrupole moment, in contrast, is characterized by *two* rate processes, a single- and a double-quantum one, with corresponding rates $W1 = 1/(2T_{1Q1})$ and $W2 = 1/(2T_{1Q2})$, respectively [1]. (The actual relaxation mechanisms, modulations of electric field gradients by Raman processes involving lattice phonons [7,8] or hyperfine interactions with electron spins [8], will not concern us here.) These two rate processes are generally of the same order of magnitude, but are not necessarily equal. Both cw-saturation as well as pulsed methods have been proposed and used to measure these individual processes in a few cases, and to relate them to theory [4,9,10]. A further complication arises from the fact that spin–lattice relaxation processes themselves can have an orientation dependence (of the crystallite with respect to the magnetic field), as discussed by Andrew et al. [11].

The present study demonstrates a useful new strategy for performing different relaxation experiments in a single-crystal (film) sample to obtain the rates for the three different processes W, $W1$, and $W2$ mentioned above. The results have been checked by comparing the behavior of two different quadrupolar isotopes of the same atom. The orientation dependence of these processes has also been investigated. One noteworthy result is that even rather small deviations of the ratio $W1/W2$ from unity can lead to significant errors, when time constants derived from good single-exponential fits to experimental data are simplistically interpreted assuming $W1 = W2$.

This work also provides a comparison between the spin–lattice relaxation of a half-integral spin in a stationary single-crystal sample and that in a polycrystalline powder sample of the same compound under magic-angle spinning (MAS). Despite the great popularity of MAS-NMR studies of half-integral quadrupolar nuclei over the past two decades, only a few reports have discussed in any detail additional complications to the measurement and interpretation of magnetization-recovery curves arising from the spinning process [12,13].

The spin-3/2 systems of interest are the ^{71}Ga (39.89% N.A.) and ^{69}Ga (60.11% N.A.) nuclei in the wide bandgap semiconductor gallium nitride, GaN. The ^{69,71}Ga spin–lattice relaxation times of several static GaN samples have been reported over a wide temperature range [14], but no attempt was made in that work to establish how closely the equality $W1 = W2$ might hold. A quadrupolar relaxation mechanism due to fluctuating electric field gradients was shown to dominate at higher temperature, especially for the sample having a lower concentration of conduction electrons. At lower temperature, especially for the more heavily doped sample, a magnetic component of the relaxation attributed to hyperfine coupling to conduction electrons was observed.

We have recently reported [15–17] unusually large shifts (up to 185 ppm) to higher frequency for ^{71}Ga and ^{14}N NMR resonances in various doped GaN samples, from the "normal" unshifted position of undoped GaN. We attributed these large shifts to Knight shifts arising from conduction electrons in the n-type doped materials. Associated with the Knight shifts is an enhancement of the spin–lattice relaxation rate, as seen originally by Korringa in metals [8] and subsequently discussed by Bloembergen [18] in semiconductors. To investigate quantitatively this association between relaxation and Knight shifts, the subject of a future paper [17], it is useful first to establish the experimental methodology for characterizing the relaxation behavior of the unshifted GaN resonances lacking measurable Knight shifts.

I will do this by comparing ^{71}Ga and ^{69}Ga relaxation behavior (for a variety of different initial conditions of the level populations of the spin system) for two samples: a static single-crystal GaN film at three different orientations and a previously characterized [19] polycrystalline sample under magic-angle spinning. The ^{71}Ga Larmor frequency is 21% greater than that of ^{69}Ga, but the nuclear quadrupole moment is 37% smaller, meaning that the relative contributions of quadrupolar and magnetic relaxation mechanisms vary significantly between isotopes. The principal axis of the axially symmetric ^{69,71}Ga quadrupole coupling tensors (and the much smaller csa tensors recently reported [15]) lie conveniently along the c-axis, normal to the plane of the film. The results from this work will be useful for reliably identifying the contributions to relaxation from conduction electrons in doped GaN samples, in addition to their broader implications for studying relaxation of quadrupolar nuclei.

The paper will be organized as follows. Section 2 will first define terminology and the starting assumptions, and give primarily previously derived theoretical results for magnetization-recovery behavior for $I = 3/2$. These results will apply for various initial conditions and for both quadrupolar, magnetic, and mixed relaxation mechanisms. These prior theoretical results apply to static samples; therefore, the additional complications introduced by the magic-angle spinning process will be considered next in the same section. In Section 3 the details of the pulse sequences used for both static and MAS situations will be presented, and some discussion will be given of the degree to which deviations from ideal initial conditions can be measured and taken into account. Section 4 will show the successful implementation of a strategy for measuring $W1$, $W2$, and W in a single crystal at various orientations, and will also show general consistency of these results with the MAS-NMR results. The dominant relaxation mechanism in the present samples will be seen to be quadrupolar, with $W1$ not necessarily equal to $W2$, and with both being orientation dependent.

2. Theoretical background

2.1. Static samples

The formal starting point for describing T_1 magnetization-recovery behavior in quadrupolar half-integral nuclei with spin I is the set of coupled linear differential equations

describing changes in the populations of the levels in terms of microscopic rate constants (transition probabilities between the levels). To render this statement more explicit, we show in Fig. 1 the energy levels and rate processes for the $I = 3/2$ system relevant here. We assume a Zeeman Hamiltonian perturbed by quadrupolar interactions to first order only, where the eigenfunctions are those of the Zeeman Hamiltonian and m is a good quantum number. The upward and downward rates (combined as a double arrow) are nearly equal, but the downward rate is greater by a factor taking into account the Boltzmann population difference between the two levels (the rate *constants* themselves are assumed equal). Finally, we assume that the spectral densities of the fluctuations responsible for the relaxation have a single value over the frequency range covering the central transition (CT) and satellite transitions (ST), i.e., that we are in the short correlation time τ_c limit where $\omega_0^2\tau_c^2 \ll 1$ (see the end of Section 4.1.1 for experimental support for this assumption).

Because of the bilinear nature of the quadrupolar Hamiltonian, both $\Delta m = \pm 1$ and $\Delta m = \pm 2$ transitions are allowed for relaxation induced by fluctuating electric field gradients (quadrupolar mechanism), with corresponding rate constants $W1$ and $W2$. Although $W1$ and $W2$ are generally of the same order of magnitude and are often assumed to be equal, they have been found to be different in at least some cases [4,9,10]. When relaxation is induced by fluctuating magnetic interactions (e.g., arising from hyperfine interactions with electron spins, anisotropic Knight or chemical shifts, or dipolar interactions with other nuclei), the corresponding transition rates are 3W and 4W, depending upon the magnetic sublevels connected. Except for avoiding using subscripts on $W1$ and $W2$, we adopt here and below the notation of Suter et al. [20], who provide a lucid description of mixed quadrupolar and magnetic relaxation processes as well as a discussion of prior work in the field (relaxation is also discussed in

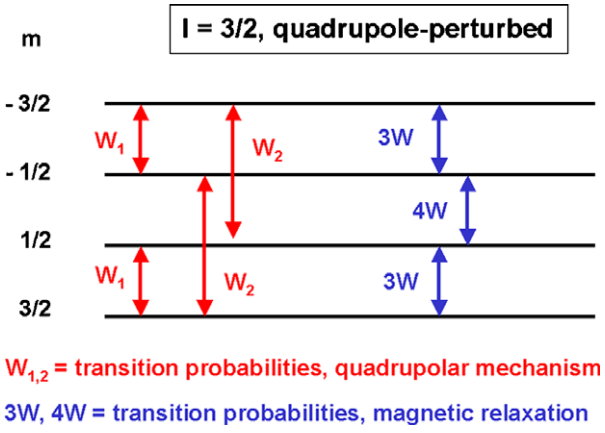

Fig. 1. Spin–lattice relaxation processes for quadrupole-perturbed $I = 3/2$ nucleus. Quadrupolar relaxation by the single-quantum process $W1$ and the double quantum process $W2$ is characterized by the two corresponding time constants T_{1Q1} and T_{1Q2}. Magnetic relaxation (e.g., by hyperfine coupling to conduction electrons or by nuclear dipole–dipole coupling) by the single-quantum process W is characterized by the time constant T_{1M}.

the excellent review of quadrupole effects in solid-state NMR by Freude and Haase [21]).

The quantity of direct interest in NMR is not the population of levels, but rather the difference in populations between adjacent levels. The equations can be solved by defining a vector $\mathbf{N}$ that corresponds to the deviation of this population difference from its equilibrium value, where N_1 corresponds to this deviation for the 3/2 and 1/2 pair of levels, N_0 for the 1/2 and −1/2 pair of levels, and N_{-1} for the −1/2 and −3/2 pair of levels (for $I = 3/2$). The reduced master equation is then given by:

$$\frac{\mathrm{d}}{\mathrm{d}t}\mathbf{N} = \mathbf{R}\mathbf{N}, \tag{1}$$

where $\mathbf{R}$ is the reduced relaxation coefficient matrix, which for the case of magnetic relaxation is given by:

$$\mathbf{R}_{\mathrm{mag}} = W\begin{bmatrix} -6 & 4 & 0 \\ 3 & -8 & 3 \\ 0 & 4 & -6 \end{bmatrix} \tag{2a}$$

and for quadrupolar relaxation by:

$$\mathbf{R}_{\mathrm{quad}} = \begin{bmatrix} -(2W1 + W2) & 0 & W2 \\ W1 - W2 & -2W2 & W1 - W2 \\ W2 & 0 & -(2W1 + W2) \end{bmatrix}. \tag{2b}$$

The set of homogeneous linear differential equations in Eq. (1) has a general solution involving the set of eigenvalues λ_i of the reduced relaxation matrix $\mathbf{R}$ corresponding to different eigenrates, as well as the eigenvectors $\mathbf{E}$ of the matrix $\mathbf{R}$. The *specific* solution of Eq. (1) depends upon the vector $\mathbf{N(0)}$ describing the initial condition of the spin system. There are two cases relevant to the present work. Case I corresponds to selective excitation of the CT, which for a selective π-pulse leads to $\mathbf{N(0)} = n_0$ [1, −2, 1], where n_0 is the population difference between adjacent levels at equilibrium. For a single or a brief series of 90° pulses that selectively saturate the CT, $\mathbf{N(0)} = n_0$ [0.5, −1, 0.5], i.e., is merely scaled by a factor of 1/2. Case II corresponds to saturation of all of the transitions, with an initial vector $\mathbf{N(0)} = n_0$ [−1, −1, −1]. The specific solutions are then given by (note that the eigenvalues λ_i are negative):

$$N_j(t) = \sum_i \left[E^{-1}\mathbf{N}(\mathbf{0})\right]_i E_{ji} \exp(t\lambda_i). \tag{3}$$

The time-dependent magnetization $M_j(t)$ for the observed transition j is then given by:

$$M_j(t) = M(\infty)\left[1 - \sum_i a_i \exp(t\lambda_i)\right] \tag{4}$$

with the coefficients a_i of the eigenrates given by:

$$a_i = -\frac{1}{n_0}\left[E^{-1}\mathbf{N}(\mathbf{0})\right]_i E_{ji}.$$

(note that these two equations differ slightly from those in Suter et al. [20], since we define $\mathbf{E}$ as a matrix having eigen-

vectors as columns rather than rows, and correct a slight typo involving subscripts for their Eq. (9)). One important point to note here is that once the eigenvectors and eigenrates are calculated for a given relaxation matrix, the effect of different initial conditions N(0) is simply to alter the *coefficients* of the individual eigenrates for a given transition being observed. Thus, as will be shown in Section 3, it is straightforward to calculate the errors introduced by non-ideal initial conditions.

Suter et al. [20] have obtained eigensolutions and the coefficients a_i for $I = 3/2$ in the mixed relaxation case, where $\mathbf{R} = \mathbf{R}_{\text{mag}} + \mathbf{R}_{\text{quad}}$, which we will not reproduce here. Although their solutions agree with previous literature values for the case of magnetic relaxation alone (i.e., in the limit that $W1,2 \to 0$), the opposite limit of pure quadrupolar relaxation ($W \to 0$) leads to coefficients with zero in the denominators. To obtain an analytic solution for the pure quadrupolar relaxation case, it is convenient to reduce the $\mathbf{R}_{\text{quad}}$ matrix from 3×3 to 2×2 by assuming symmetrical initial conditions for the two satellite transitions ST, so that $N_1 = N_{-1}$. For the population deviation vector $[N_1,\ N_0]$ the relaxation matrix is:

$$\mathbf{R}_{\text{quad}} = \begin{bmatrix} -2W1 & 0 \\ 2(W1 - W2) & -2W2 \end{bmatrix} \tag{5}$$

and there are two eigenvalues, $-2W1$ and $-2W2$ along with the matrix $\mathbf{E}$ of eigenvectors as columns (which coincidentally is equal to its own inverse):

$$\mathbf{E} = \begin{bmatrix} -1 & 0 \\ 1 & 1 \end{bmatrix}. \tag{6}$$

As Andrew and Tunstall [2] showed, for all initial population differences zero (complete saturation of all transitions) the CT recovers as:

$$M(t) = M_0[1 + \exp(-2[W1]t) - 2\exp(-2[W2]t)]. \tag{7}$$

We can easily show from the preceding that for the same initial conditions, the ST by contrast recovers with a *single*-exponential rate constant of $2W1$. Gordon and Hoch [4] provided numerical solutions for pure quadrupolar relaxation for spins 3/2 to 9/2, for initial conditions of either complete saturation, a long CW or comb saturation, or for a selective pulse on one transition (CT). For $I = 3/2$, single-exponential recovery for the CT was observed for all initial conditions only when $W1 = W2$, when Eq. (7) reduces to a single-exponential recovery. Otherwise, the behavior could deviate strongly from single-exponential, and it depended upon both the ratio of $W2/W1$ and the initial conditions. For the selective CT pulse, their analytical solution for the CT intensity (identical to that cited by Corti et al. [14]) is:

$$M(t) = M_0[1 - 0.5\ \exp(-[2W1]t) - 0.5\ \exp(-[2W2]t)], \tag{8}$$

as can be readily derived from the preceding discussion. Finally, for completeness we note that McDowell [22] has given explicit relaxation matrices for up to $I = 9/2$ for the case of magnetic relaxation and provides a general discussion.

2.2. Samples with MAS

The preceding discussion involved only static samples. Woessner and Timken [12] discussed the influence of magic-angle spinning (MAS) upon spin–lattice relaxation behavior of half-integer spins, and gave experimental results for ^{27}Al ($I = 5/2$). They discuss at length two important points relevant to the present experiments. First, they note that when a comb (long train) of saturation pulses centered at the CT (with an excitation width considerably smaller than the width of the ST pattern) is applied to a spinning sample, the ST will also likely be saturated as well. This arises as a result of the fact that the ST for each crystallite varies in frequency during the rotor period, and crosses zero frequency (the CT) several times, making it highly probable that it will be affected by a saturating pulse arising near that crossing (this assumes that the saturating pulse train is *asynchronous* with rotor spinning; otherwise, most ST will not be affected). Second, they noted that these zero-crossings of the ST (when the frequencies of the ST and CT match within the homogeneous linewidth due to homonuclear dipolar couplings) allow mutual spin-flips (cross-relaxation, or spin-exchange) with the CT. When a single-saturating pulse is used rather than a comb, the result is that the T_1 recovery is much faster (and non-exponential) under MAS compared to the static case, since the ST population differences can be transferred to the CT by cross-relaxation. Similar, albeit even more marked, effects have been noted recently [13], and discussed in terms of rotational resonance. This work noted that the rotational resonance condition was reduced or eliminated by spinning away from the magic angle (when second-order shifts were small). In a sample where the second-order quadrupolar broadening of the CT was significant, the rotational resonance condition was not met at the magic-angle, but could be partially met by spinning away from the magic-angle. Rotational resonance was shown to shorten by nearly two orders of magnitude the inversion recovery time of the central transition, and it was suggested that this might offer sensitivity advantages [13]. However, this marked reduction appears to be a consequence of population transfer from presumably equilibrated satellite transitions, and hence is not sustainable for steady-state rapid pulsing on the central transition. Another consequence of rotational resonance is a shortening of the T_2 relaxation time, leading to the surprising consequence that spinning slightly away from the magic-angle actually resulted in a sharper CT.

3. Experimental

3.1. MAS-NMR experiments

A 500 MHz (^{1}H) Bruker Avance DMX spectrometer was used. For MAS experiments a 4 mm triple-resonance CPMAS probehead was used in double-resonance mode (without plug-in insert). The sample was polycrystalline hexagonal GaN synthesized and characterized by ^{71}Ga and ^{14}N MAS-NMR as described previously [19]. The 90° pulse lengths for the ^{71}Ga (152.575 MHz) and ^{69}Ga (102.077 MHz) central transitions were 2.3 and 2.4 μs, respectively, and the total spectral width was 1.667 MHz. The spinning speed was set to 9.000 kHz and controlled within ±1 Hz. The effect of spinning speed on sample temperature was measured using a lead nitrate chemical shift "thermometer" [23]; a 9 °C rise above ambient temperature at a spinning speed of 9.0 kHz was measured and used to correct the sample temperature.

Saturation of all satellite transitions as well as the central transition was accomplished by applying a train of 60 pulses (corresponding to 90° pulses for the central transition) at intervals of 2.01 ms; since this interval corresponds to 18.09 rotor periods, the effect is to "step through" the rotor period in 9% increments and thus saturate the satellite transitions of all crystallites at some time or another. Since the saturating pulses are not delta pulses but instead have a width that is 3% of the rotor period, frequency changes during the pulses can complicate the behavior, depending upon the individual crystallite orientation. The most likely effect is that some crystallites will experience effective flip angles less than 90° due to their being outside the excitation bandwidth during some portion of the pulse. Adiabatic passage considerations are less likely to be influential because of the short pulse widths. Although detailed numerical simulation of the saturation behavior for $I = 3/2$ for a given NQCC and (asymmetry parameter) as a function of rf field strength, spinning speed, and number, spacing and length(s) of saturating pulses might be informative, if somewhat laborious, a practical solution (used here) is to monitor the intensities of the satellite transitions for the shortest possible recovery time, to ensure that adequate saturation is achieved (in this case, reduction of the satellite intensities to somewhere less than 1/16 of their original value was observed; signal:noise limitations precluded obtaining a more precise value).

Following the last saturation pulse, a variable recovery period was allowed, and the signal was then obtained using a 90°–τ–180°–τ Hahn echo with each interval (including half-widths of pulses) set equal to the rotor period. Experiments with different recovery times were not interleaved, since the number of scans accumulated was set to be larger for the shorter recovery times (this was also true for the static film experiments). Instead, the stability of the spectrometer system was checked by inserting repeated measurements for a given recovery time, and found to be constant within about ±1% for the data sets analyzed. An exponential line-broadening of 100 Hz was applied to the signal starting at the echo maximum, and the intensities of individually phased spectra were measured relative to a fully relaxed spectrum using the scaling factor from the XWINNMR dual-display feature. This procedure has the advantage of revealing any subtle changes in lineshape that might result from differential relaxation or other effects.

3.2. Static single-crystal (film) experiments

The static ^{69}Ga and ^{71}Ga NMR spectra were obtained on a high-power variable-temperature broadband probe with a high-Q insert and a home-built 15 mm wide 7-turn flat coil containing the GaN film in a holder made from a flat clear plastic file-tab. The coil is basically a solenoid that has been flattened but that encloses the flat sample and holder. Thus, the rf field is still along the original axis of the solenoid coil. As a result, the coil can be physically reoriented to achieve different orientations of the quadrupole coupling tensor symmetry axis (which lies along the crystallographic *c*-axis, normal to the film) with respect to the magnetic field, with minimal change in rf field strength. The transparent film was a commercial sample grown by hydride vapor phase (HVPE) ca. 250 μm thick and 10 × 10 mm square, or a triangular fragment thereof, whose NMR characteristics closely resemble those of a previously studied hexagonal-GaN film [15]. The temperature measured by a thermocouple in the probe (with a slow flow of ambient nitrogen gas for cooling purposes) remained between 296 and 298 K, and relaxation delays of 0.2 s were used to reduce possible sample heating by rf pulses in experiments with short saturation-recovery times.

The probe was tuned and matched for the CT peak in all cases, even when the carrier frequency was set at a ST frequency. A pulse program was written to apply a cycle of 90° saturation pulses from a list at various frequency offsets spaced at 2 ms intervals (to allow transverse signal to decay fully), returning to the final observation frequency with an offset of 0 Hz in the list. The actual offset ("O1" in XWINNMR) was set to place either the CT or the desired ST at the carrier frequency; this was necessary, since large frequency offsets used *within* a list are apparently not phase coherent as needed for signal-averaging purposes, but are nevertheless effective for saturation purposes. An example is the sequence used to measure ^{71}Ga CT(all-sat) recovery for the perpendicular tensor symmetry axis orientation (as defined in Section 4.1.1, CT(all-sat) refers to observation of the central transition CT for initial conditions of all transitions saturated; "sel-sat" is also defined there to correspond to selective saturation). In this case, a 90° pulse for the CT of 10 μs was used, and the average 90° pulse for the ST (measured by changing the carrier frequency to be on-resonance with the ST, but without retuning the probe) was 12.2 μs. From an "O1" offset corresponding to an on-resonance CT, the appropriate 90° pulses were applied to ST and CT with the following offsets: $(+430.7\text{ kHz}, -430.7\text{ kHz}, 0)_5$, where the subscript indicates that the

cycle of three saturating pulses was repeated five times. As a check of the efficacy of this saturation procedure, the peak heights for a minimal 2 ms recovery (where only ca. 0.05% of the fully saturated magnetization recovers) were compared to those of a fully recovered spectrum. The measured values were 1.0% (CT), 2.4% (left ST), and 5.2% (right ST). In general, this procedure could be used to set the *exact* initial conditions for calculating recovery curves, as described in Section 2. However, in the present experiments, the measured deviations were generally less than a few percent, and were shown by explicit calculation for the most non-ideal case not to have a measurable effect (viz. less than 0.2%) on the predicted recovery curves. This insensitivity to deviations from the ideal saturation initial conditions results from the fact that the two individual eigenrates do not differ by a large amount; in cases where they did, incorporating actual experimentally determined initial conditions would be sensible. The procedures used for this and the remaining ^{71}Ga as well as the ^{69}Ga saturation-recovery experiments are given in Table 1.

One should note that the above discussion implicitly assumes a uniform B_1 field and hence uniform flip-angles for the entire sample. Any significant B_1 inhomogeneity would lead to partial cancellation of signals following a final nominal 90° pulse from different portions of the sample having either a $+z$ or $-z$ component of magnetization. Although not implemented here, using saturating pulses of variable length (e.g., 80°, 90°, and 100°) would obviate this potential problem.

Because the *c*-axis of hexagonal GaN is normal to the film plane, when this normal is perpendicular to the external magnetic field the quadrupole coupling tensor symmetry axis (and small csa tensor symmetry axis) are also perpendicular. The sample orientation with respect to the external magnetic field was deduced from the magnitude of the ST splittings, which are reflected in the frequency offsets in Table 1. Using the known values of the nuclear quadrupole coupling constants NQCC [15], the accuracy of the perpendicular tensor symmetry axis orientation is ca. ±2°, whereas that of the parallel orientation is ca. ±6°. As discussed in Section 4, the magic-angle tensor symmetry axis orientations were much more accurate.

The peak intensities (an appropriate exponential apodization function was applied before Fourier-transformation) were measured relative to that of a relaxed spectrum using the dual display feature of XWINNMR. Since a good signal:noise ratio (typically 500:1) was obtained, the errors in measuring peak intensities were most likely determined by spectrometer drift, and as mentioned above the overall error is estimated as roughly ±1%, which corresponds to the width of the experimental points in the figures. The data analysis program Origin 7.0 was used for fitting saturation-recovery data to the defined relaxation functions obtained from solving the analytical expressions using a MATLAB script.

4. Results and discussion

4.1. Static film sample

4.1.1. General strategy

Since this paper considers samples where the quadrupolar mechanism is the dominant, but not sole, factor in relaxation of ^{69,71}Ga nuclei, Fig. 2 provides a useful illustration of the CT saturation-recovery behavior (according to Eq. (7)) for several combinations of the quadrupolar time constants T_{1Q1} (=1/[2W1]) and T_{1Q2} (=1/[2W2]) when all transitions are initially saturated. When T_{1Q1} is sufficiently larger than T_{1Q2} (e.g., 5 s vs. 3 s) we see that the magnetization recovery exhibits an overshoot, exceeding 100% of the CT final magnetization. When T_{1Q1} is sufficiently smaller than T_{1Q2} (e.g., 1 s vs. 3 s), the magnetization recovery actually exhibits a negative-going dip. When T_{1Q1} is only slightly larger than T_{1Q2} (4 s vs. 3 s) the calculated recovery curve appears to be reasonably close to single-exponential; forcing a fit of this curve to a single-exponential gives a time constant T_1 ($\equiv T_{1Q1} = T_{1Q2}$) = 2.2 s. The expanded difference plot shows that the calculated recovery curve agrees within a couple of percent of that for a single-exponential; however, the corresponding time constants are substantially different, with T_{1Q1}, $T_{1Q2} > T_1$. These simulations clearly demonstrate that even though experimental relaxation curves may closely approximate single-exponential recovery,

Table 1
Experimental conditions for saturation-recovery measurements (see Section 3)

Nucleus, NQCC tensor symmetry axis orientation	CT(all-sat) (offset in kHz)	CT(sel-sat) (offset in kHz)	ST(all-sat) (offset in kHz)	Pulse widths (μs)
^{71}Ga, perpendicular	$(+430.7, -430.7, 0)_5$	$(0, 0, 0)_1$	$(0, -864, -432)_5$	$(12.2, 12.2, 10)_n$[c]
^{71}Ga, parallel	$(+847.5, -847.5, 0)_5$	—	$(0, -1695, -847.5)_5$	$(3.85, 3.85, 2.0)_n$
^{71}Ga, magic-angle	$(0)_{20}$	Not achievable	$(0)_{20}$	$(4.3)_n$
^{69}Ga, perpendicular	$(+682.5, -682.5, 0)_8$	$(0)_2$[a]	$(0, -1365, 0)_8$[b]	$(4.35, 4.35, 3.0)_n$
^{69}Ga, magic-angle	$(0)_6$	Not achievable	$(0)_6$	$(5.4)_n$

[a] 90° pulse for CT = 12.5 μs.
[b] CT inadvertently excluded from list; nevertheless, CT saturation measured to be 89% of full saturation, with negligible calculated effects on recovery curves.
[c] The rf strength of the pulses used here was set to be less than that for the pulses below in the table, since selective excitation of the CT was desired.

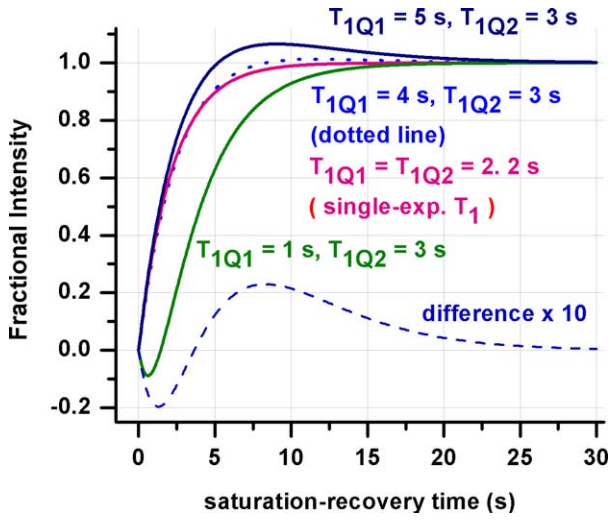

Fig. 2. Magnetization-recovery curves for the central transition of $I = 3/2$ for the initial condition of all transitions saturated, "CT(all-sat)," and a purely quadrupolar mechanism, calculated using Eq. (7). Note the nearly indistinguishable recovery curves for the two quite different cases $T_{1Q1} = 4$ s, $T_{1Q2} = 3$ s, and T_{1Q1}=$T_{1Q2} = 2.2$ s, illustrating the potential inaccuracies in relaxation times that can result from an apparently good fit to a single-exponential curve.

assuming that form may lead to substantial errors in the relaxation parameters.

A simple way of estimating the single best-fit T_1 value (which is not rigorously defined, since it depends on how many long-time points are included in the fit) is given by $T_1 \approx 2T_{1Q2} - T_{1Q1}$. This approximation works to better than about 12% over the range $T_{1Q1} = 4$ s, $T_{1Q2} = 3$ s to $T_{1Q1} = 3$ s, $T_{1Q2} = 4.5$ s, just to give easily understood numerical values that can be scaled to any other actual values. Note that when $T_{1Q1} < T_{1Q2}$, the best-fit T_1 will be *larger* than either of the two values. If only shorter time data are considered for the fits, then the first term in the series expansion of the exponential yields the result $T_1 \approx (T_{1Q1}T_{1Q2})/(2T_{1Q1} - T_{1Q2})$.

The strategy adopted here is to measure more reliable relaxation parameters by carrying out three experiments each for ^{71}Ga and ^{69}Ga in a given film orientation: (1) CT(all-sat), (2) ST(all-sat), and (3) CT(sel-sat). Experiments (1) and (2) refer to initial conditions of complete saturation of all transitions, achieved by a series of frequency-jumped 90° pulses on both the central transition CT and the pair of satellite-transitions ST, and differ only in whether the CT (Experiment 1) or the ST (Experiment 2) is observed. Experiment 3 refers to observation of the central-transition CT after it is excited by a small number of relatively weak 90° pulses, that do not excite the ST. Thus, a total of six ^{69,71}Ga experiments were carried out with a film orientation yielding the *c*-axis (normal to the film) perpendicular to the external magnetic field, and will be discussed beginning in the next subsection; results from a smaller number of experiments at two other film orientations will be discussed in following subsections.

Finally, the assumption made in Section 2 of relaxation being in the short correlation time limit where $\omega_0^2\tau_c^2 \ll 1$, quite reasonable for a rigid tetrahedrally bonded partly ionic solid like GaN, is supported by relaxation results at two different field strengths for the parallel tensor symmetry axis orientation of film #1 in [15]. Fitting CT(sel-sat) results to a single-exponential time constant gave a value of 4.26 s at 11.7 T and 3.51 s at 7.0 T. Although these values are not exactly equal, as would be the case in the short correlation time limit, for the long correlation time limit there would be a quadratic dependence of the relaxation time upon field strength and thus a predicted time constant at the higher field of 9.75 s instead of the observed 4.26 s.

4.1.2. ^{69,71}Ga results, perpendicular tensor symmetry axis orientation

The ^{71}Ga results for the perpendicular tensor symmetry axis orientation are given in Figs. 3–5 for the CT(all-sat), ST(all-sat), and CT(sel-sat) saturation-recovery experiments. The ^{71}Ga ST(all-sat) results shown in Fig. 4 could be fit to a single-exponential recovery with a time constant = 3.57 s. If one makes the starting assumption that the relaxation is entirely quadrupolar in origin, then Section 2 above indicates that only the $W1$ rate process contributes to this recovery curve, and thus $T_{1Q1} = 3.57$ s. The ^{71}Ga CT(all-sat) results shown in Fig. 3 can also be fit to a single-exponential recovery, but the corresponding time constant of 2.82 s is different, and thus inconsistent with any assumption that $T_{1Q1} = T_{1Q2}$ (this can be readily seen from Eq. (7) for the case of purely quadrupolar relaxation, and can also be shown to be true when magnetic relaxation contributes [20]). Therefore, we make again the starting assumption that relaxation is entirely quadrupolar

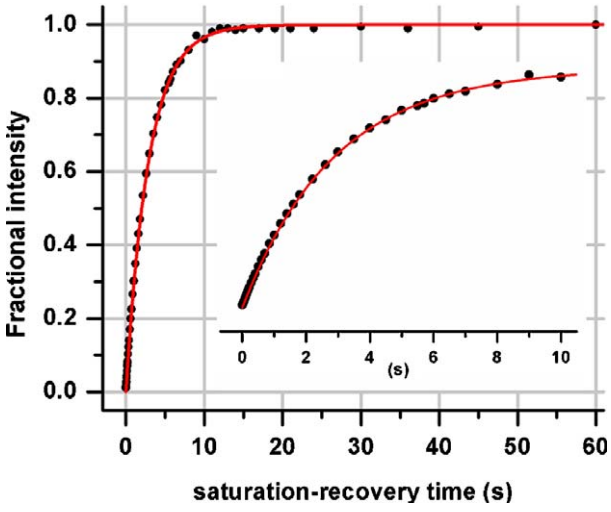

Fig. 3. ^{71}Ga magnetization recovery of the central transition with all transitions saturated initially, "CT(all-sat)," for a GaN film with the nuclear quadrupole coupling tensor symmetry axis (lying along the *c*-axis, which is normal to the film plane) oriented perpendicular to the field. The theoretical curve was calculated as described in the text, from the appropriate two eigenrates and eigencoefficients calculated using the parameters $T_{1Q1} = 3.85$ s, $T_{1Q2} = 3.42$ s, and $T_{1M} = 49$ s.

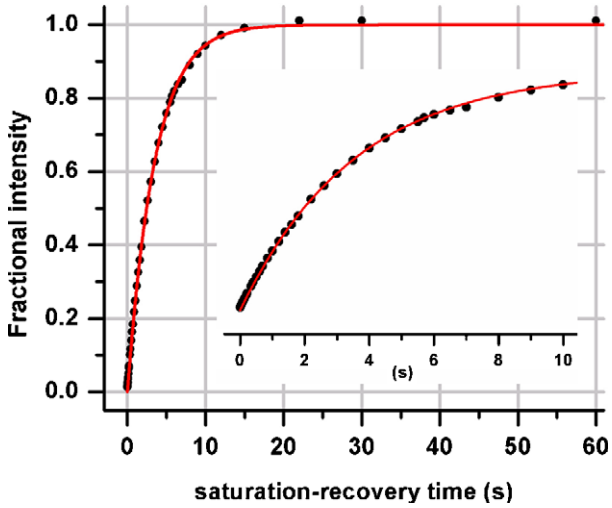

Fig. 4. ^{71}Ga magnetization recovery of the high-frequency satellite transition with all transitions saturated initially, "ST(all-sat)," for a GaN film with the nuclear quadrupole coupling tensor symmetry axis oriented perpendicular to the field. The theoretical curve was calculated as described in the text, from the appropriate two eigenrates and eigencoefficients calculated using the same parameters as for Fig. 3.

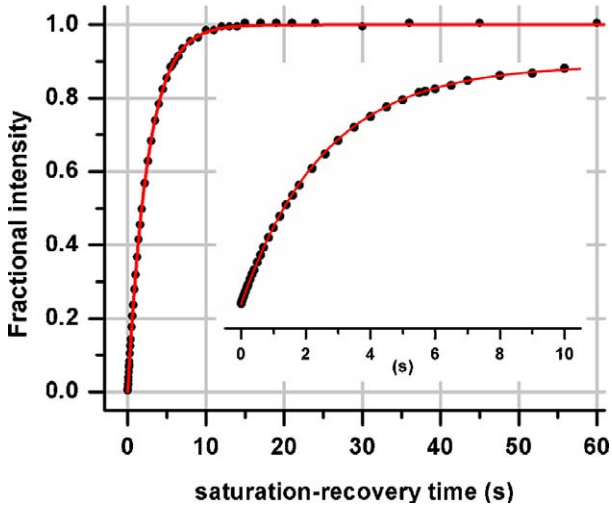

Fig. 5. ^{71}Ga magnetization recovery of the selectively saturated central transition, "CT(sel-sat)," for a GaN film with the nuclear quadrupole coupling tensor symmetry axis oriented perpendicular to the field. The theoretical curve was calculated as described in the text, from the appropriate two eigenrates and eigencoefficients calculated using the same parameters as for Fig. 3.

in origin, fit the data using Eq. (7) with $T_{1Q1} = 3.57$ s as obtained from the ST(all-sat) results, and obtain $T_{1Q2} = 3.17$ s as the best fit.

However, the CT(sel-sat) data shown in Fig. 5, when fit to Eq. (8) describing the recovery for an entirely quadrupolar relaxation mechanism, yield $T_{1Q1} = 2.87$ s, $T_{1Q2} = 2.41$ s, in significant disagreement with the above values. Thus, the contribution from magnetic relaxation (presumably by hyperfine interaction with conduction electrons) can be considered to be small but non-negligible in these experiments. To take it into account quantitatively, we need to use Eq. (4) and the analytical expressions for eigenrates and eigencoefficients given by Suter et al. [20]. This becomes a very difficult fitting problem, since these rates and coefficients defining the form of the recovery function depend upon the three unknowns W, $W1$, and $W2$. However, we can recognize that the previous results provide a reasonable estimate of the relative sizes of T_{1Q1} and T_{1Q2} (or $W1$ and $W2$); if we fix their values, then only if the magnitude of T_{1M} (relative to T_{1Q1} or T_{1Q2}) changes do the eigenrates and eigencoefficients change. In other words, we can allow the value of W to assume a range of trial values, and calculate the eigenrates and eigencoefficients for each value. (For the relaxation experiments performed, only two eigencoefficients were non-zero, and thus only two eigenrates were needed.) To compare calculated with experimental recovery curves, however, introducing an overall scaling constant for the eigenrates that could be varied in the fitting procedure was the most useful approach. In effect, the *relative* sizes of W, $W1$, and $W2$ were fixed in a given trial (to give a set of eigenrates/eigencoefficients), but the absolute rate constants were varied by this scaling factor. To the degree that the best-fit scaling factor in all three experiments turned out to be identical, the results can be considered to be internally consistent. A number of different starting values with differing ratios of T_{1Q1} to T_{1Q2} were tried with a variety of T_{1M} values, but the best results overall (including fitting the ^{69}Ga data as described below) were obtained starting with the original $T_{1Q1} = 3.57$ s, $T_{1Q2} = 3.17$ s, and a value of T_{1M} (=1/[2W]) of 45 s. The resultant best-fit scaling factors for the eigenrates were 0.9569, 0.9168, and 0.907 for the CT(all-sat), ST(all-sat), and CT(sel-sat) experiments, respectively. These values are slightly less than 1, as expected, since the starting $T_{1Q1,2}$ values assumed entirely quadrupolar relaxation, and hence overestimated the corresponding rate constants slightly. They are also close to each other, being within 3% of the average scaling factor of 0.9269. Therefore, this *average* scaling factor for the eigenrates was used to calculate theoretical curves for all three experiments, with only the signal amplitude allowed to vary, as shown in Figs. 3–5. These simulations thus represent the predicted recovery curves for an internally consistent set of values $T_{1Q1} = 3.85$ s, $T_{1Q2} = 3.42$ s, and $T_{1M} = 49$ s, which are given in Table 2. The agreement with the experimental data is remarkably good, at both short times as shown in the insets and at long times. In contrast, note that while blithely fitting the recovery curves to a *single-exponential* time constant yields good fits with constants of 2.82 s for CT(all-sat), 3.57 s for ST(all-sat), and 2.63 s for CT(sel-sat), these constants have no direct physical significance except that for the ST(all-sat) experiment, which equals T_{1Q1}. (An analogous statement holds true for the ^{69}Ga results discussed in the next paragraph.)

Having obtained good self-consistent values for T_{1Q1}, T_{1Q2}, and T_{1M} for ^{71}Ga in this GaN sample with the tensor(s) symmetry axes oriented perpendicular to the field, a further check of self-consistency is provided by the

Table 2
Quadrupolar and magnetic relaxation time constants obtained from single-crystal (film) analysis (see Section 4 for details)

Nucleus, NQCC tensor symmetry axis orientation	T_{1Q1} (s)	T_{1Q2} (s)	T_{1M} (s)
^{71}Ga, perpendicular	3.85	3.42	49
^{69}Ga, perpendicular	1.53[a]	1.36[a]	78[a]
^{71}Ga, parallel	4.54	3.44	48
^{71}Ga, magic-angle	3.75	3.79	49
^{71}Ga, magic-angle	3.90[b]	3.90[b]	31[b,c]
^{69}Ga, magic-angle	1.54[b]	1.54[b]	51[b,c]

[a] Values calculated based on ^{71}Ga results and used for fits.
[b] Values obtained by assuming $T_{1Q1} = T_{1Q2}$ at this orientation, and solving simultaneous equations for ^{71}Ga and ^{69}Ga recovery.
[c] The differences between these values and other values in the table most likely result from the error range of the analysis procedure for this much smaller contributing process, rather than from any anisotropy in T_{1M}.

^{69}Ga data shown in Figs. 6–8. We can scale the values of $T_{1Q1,2}$ arising from the quadrupolar mechanism by the *inverse square* of the corresponding quadrupole moments, to obtain $T_{1Q1}(^{69}\text{Ga}) = 1.530$ s, $T_{1Q2}(^{69}\text{Ga}) = 1.358$ s (the ratio of ^{69}Ga to ^{71}Ga nuclear electric quadrupole moments has been redetermined [24] to be 1.586833, only slightly different from the earlier reported value). We can scale the value of T_1 arising from the magnetic relaxation mechanism by the inverse square of the corresponding magnetogyric ratios to obtain $T_{1M}(^{69}\text{Ga}) = 78.4$ s. Putting these predicted values (listed in Table 2) into the analytical expressions [20] yields the fits shown in Figs. 6–8, with the signal amplitude as the only fitting variable. The agreement is reasonably good, especially considering that the relaxation parameters were totally derived from the ^{71}Ga results, and that the quadrupolar contribution for ^{69}Ga is significantly larger than for ^{71}Ga, whereas the opposite holds true for the magnetic contribution to relaxation.

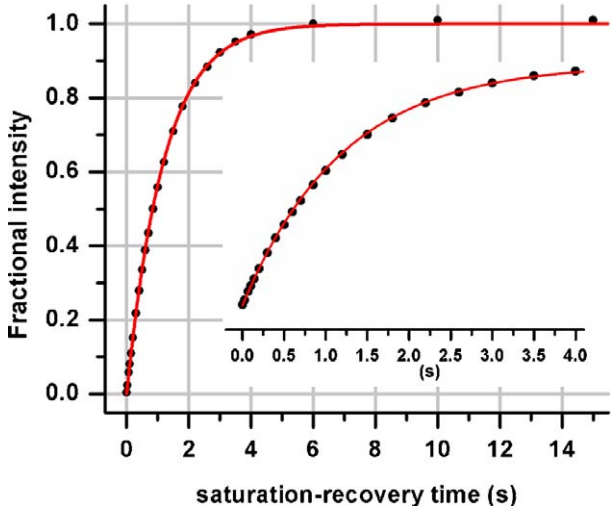

Fig. 6. ^{69}Ga magnetization recovery of the central transition with all transitions saturated initially, "CT(all-sat)," for a GaN film with the nuclear quadrupole coupling tensor symmetry axis oriented perpendicular to the field. The theoretical curve was calculated as described in the text, from the appropriate two eigenrates and eigencoefficients calculated using the parameters of Fig. 3 after scaling for the difference in magnetic moments and nuclear quadrupole moments of the two isotopes (see text).

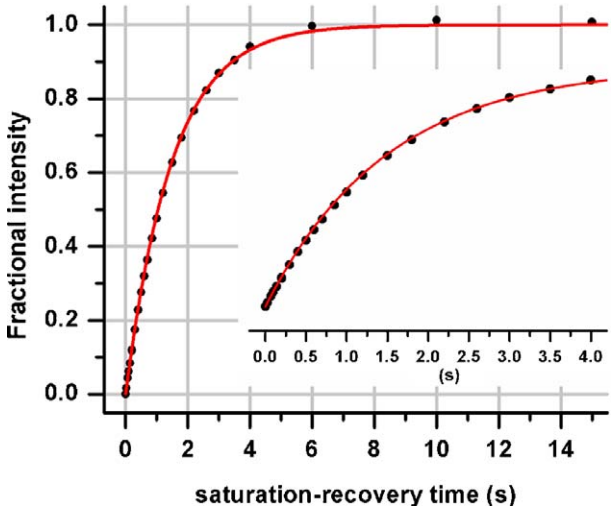

Fig. 7. ^{69}Ga magnetization recovery of the high-frequency satellite transition with all transitions saturated initially, "ST(all-sat)," for a GaN film with the nuclear quadrupole coupling tensor symmetry axis oriented perpendicular to the field. The theoretical curve was calculated as described in the text, from the appropriate two eigenrates and eigencoefficients calculated using the parameters of Fig. 6.

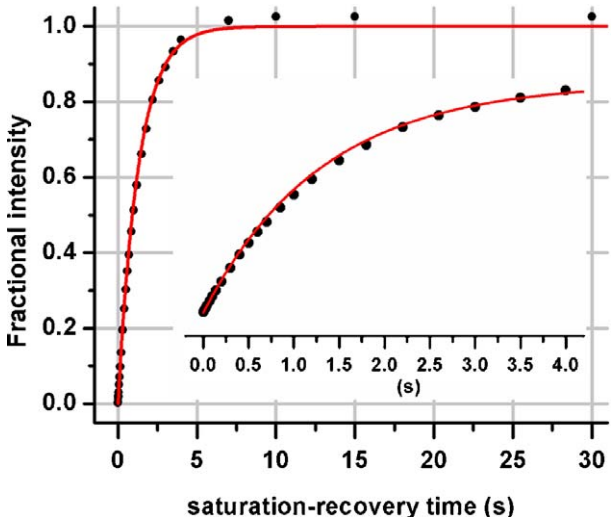

Fig. 8. ^{69}Ga magnetization recovery of the selectively saturated central transition, "CT(sel-sat)," for a GaN film with the nuclear quadrupole coupling tensor symmetry axis oriented perpendicular to the field. The theoretical curve was calculated as described in the text, from the appropriate two eigenrates and eigencoefficients calculated using the parameters of Fig. 6.

Unfortunately one cannot readily assign simple error bars to the relaxation parameters because of the multivariate nature of the analysis. Some indication of the accuracy of the values can be obtained by comparing the three theoretical curves for the parameters used in fitting Figs. 3–5 ($T_{1Q1} = 3.85$ s, $T_{1Q2} = 3.42$ s, and $T_{1M} = 49$ s) with those resulting from varying one parameter at a time. Thus,

increasing T_{1Q1} to 4.25 s leads to differences of up to 3% between the two recovery curves, which represents a systematic difference well outside the estimated errors of ca. ±1%. Decreasing T_{1Q1} to 3.65 s (near equality with T_{1Q2}) also results in systematic discrepancies of up to 5%. Similarly, decreasing T_{1M} to 35 s results in systematic discrepancies of up to 4%, and increasing it to 60 s produces discrepancies of 2%. Obviously the relative accuracy of the T_{1Q1} and T_{1Q2} values is much greater than that of the significantly longer T_{1M} value. It appears reasonable that T_{1Q1} is some 13% larger than T_{1Q2} for this perpendicular tensor symmetry axis orientation, from the unsuccessful attempts to obtain fits to all of the data trying other ratios. The solution obtained is almost certainly near a *unique* one, rather than constituting a local but not global minimum, since as Fig. 2 shows the recovery curves depend strongly on relative $T_{1Q1,2}$ values for the case of all-quadrupolar relaxation. Overall, one can conclude that making T_{1Q1} slightly larger than T_{1Q2}, and taking into account a much longer T_{1M}, has provided a way to reconcile experimental results that would otherwise be inconsistent.

4.1.3. ^{71}Ga results, parallel tensor symmetry axis orientation

All of the results discussed up to this point have been for a sample having a tensor symmetry axis orientation perpendicular to the magnetic field, which for a powder sample represents the most probable orientation. However, it is of interest to consider how the relaxation times T_{1Q1} and T_{1Q2} may depend upon the tensor symmetry axis orientation. Therefore, a less detailed study of the parallel tensor symmetry axis orientation (film perpendicular to the field) was carried out. The ^{71}Ga CT(all-sat) and ST(all-sat) recovery curves could be fit to single-exponential constants of 2.52 s and 4.23 s, respectively (data not shown). Using the latter value as a starting estimate for T_{1Q1}, and estimating T_{1Q2} as 3.20 s from Eq. (7) as described previously, I then used the analytical expressions for eigenrates and eigencoefficients [20] assuming that the magnetic contribution T_{1M} was the same as that in the perpendicular tensor symmetry axis orientation. By the same procedure described above, the "best" values obtained were $T_{1Q1} = 4.54$ s, $T_{1Q2} = 3.44$ s, and $T_{1M} = 48$ s, as given in Table 2, with the agreement between theoretical and experimental curves being excellent. It is interesting to note that although T_{1Q2} and T_{1M} are essentially identical to that determined for the perpendicular tensor symmetry axis orientation, T_{1Q1} has increased significantly, and is now some 32% larger than T_{1Q2}. Also, the experimental situation for this parallel tensor symmetry axis orientation is very similar to the illustrative CT(all-sat) saturation-recovery curve for the quadrupolar mechanism alone with $T_{1Q1} = 4$ s and $T_{1Q2} = 3$ s depicted in Fig. 2, where a single-exponential recovery with a significantly shorter time constant (=2.2 s) fits fairly closely the calculated curve.

4.1.4. ^{69,71}Ga results, "magic-angle" tensor symmetry axis orientation

The GaN film was also oriented by changing the orientation of the flat coil such that the quadrupole tensor symmetry axis was aligned very close to the "magic-angle" of 54.7356° (from the ST splitting of ca. 15 kHz seen in Fig. 9A, the actual angle is 0.4° *on either side of* the exact M.A.). As expected for the case of *non-selective* rf pulses affecting both CT and ST simultaneously, the 90° pulse lengths for both were approximately twice as long as for the *selective* case for the parallel and perpendicular tensor symmetry axis orientations, and thus corresponded to a "solution" 90° pulse length. Also note that the ST transitions are not symmetrical about the CT due to differing second-order shifts (see below). Due to the closeness of spacing and partial overlap of the ST with the CT, no frequency-shifting was necessary during the train of twenty 90° pulses used to saturate all transitions, and the recovery of both the CT and ST could be monitored from the same spectrum (the better-resolved ST to high-frequency was monitored). The experimental recovery curves for both CT(all-sat) and ST(all-sat) are shown in Figs. 10 and 11, and fit well to single-exponential time constants of 3.56 and 3.48 s, respectively (fits not shown). Using the same procedure as above, I set the latter time constant to equal the "starting" T_{1Q1}, and fit the CT recovery to Eq. (7) to obtain a "starting" $T_{1Q2} = 3.52$ s. These values were then combined with a "starting" T_{1M} value of 45 s, and the analytical expressions [20] were used to calculate eigenrates and eigencoefficients. The resultant rate scaling factors

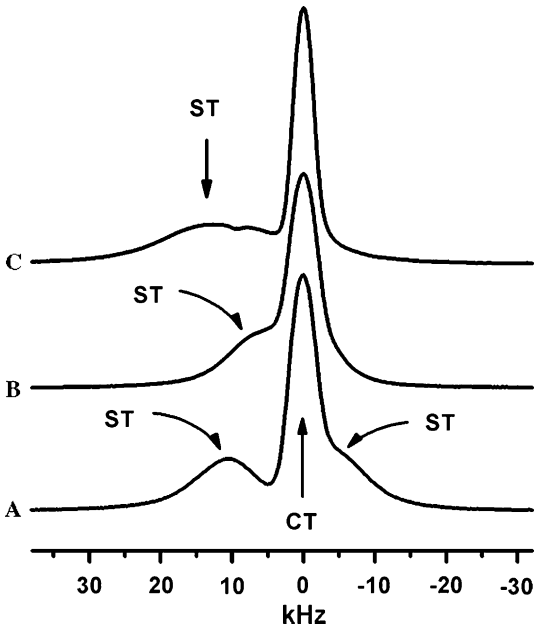

Fig. 9. ^{71}Ga (A and B) and ^{69}Ga (C) spectra for GaN film with nuclear quadrupole coupling tensor symmetry axis oriented very near (A) or exactly at (B and C) the "magic-angle." The central transitions are labeled "CT," and were assigned zero frequency, and satellite transitions are labeled "ST." An exponential apodization corresponding to a line-broadening of 200 Hz was applied in all cases.

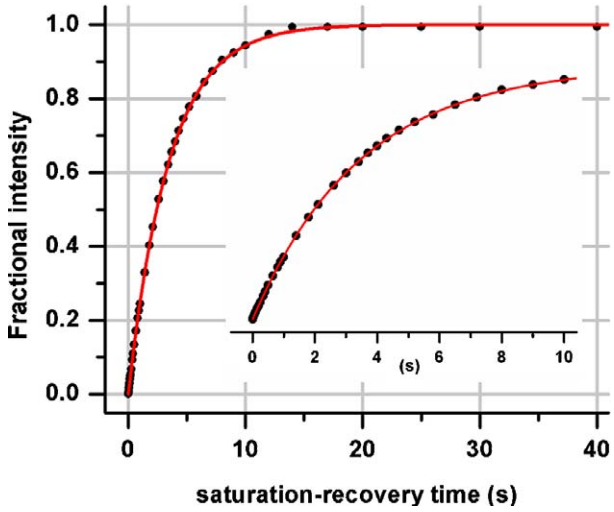

Fig. 10. ^{71}Ga magnetization recovery of the central transition with all transitions saturated initially, "CT(all-sat)," for a GaN film with the nuclear quadrupole coupling tensor symmetry axis oriented with respect to the field at 0.4° away from the "magic-angle." The theoretical curve was calculated as described in the text, from the appropriate two eigenrates and eigencoefficients calculated using the parameters $T_{1Q1} = 3.75$ s, $T_{1Q2} = 3.79$ s, and $T_{1M} = 49$ s.

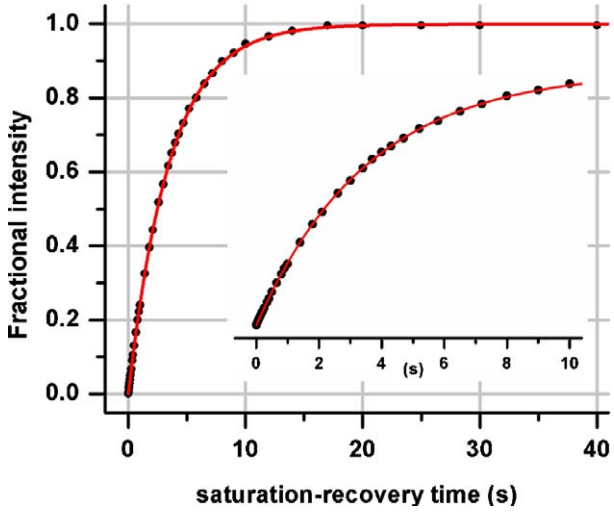

Fig. 11. ^{71}Ga magnetization recovery of the high frequency satellite transition with all transitions saturated initially, "ST(all-sat)," for a GaN film with the nuclear quadrupole coupling tensor symmetry axis oriented with respect to the field at 0.4° away from the "magic-angle." The theoretical curve was calculated as described in the text, from the appropriate two eigenrates and eigencoefficients calculated using the same parameters as for Fig. 10.

from the two fits were nearly identical, and the average scaling factor was then used to calculate the recovery curves shown in Figs. 10 and 11, using $T_{1Q1} = 3.75$ s, $T_{1Q2} = 3.79$ s, and $T_{1M} = 49$ s (values listed in Table 2). The agreement with the experimental curves is excellent. At this near-magic-angle orientation the T_{1Q1} and T_{1Q2} values are essentially equal, unlike the perpendicular and especially the parallel tensor symmetry axis orientations (Fig. 12).

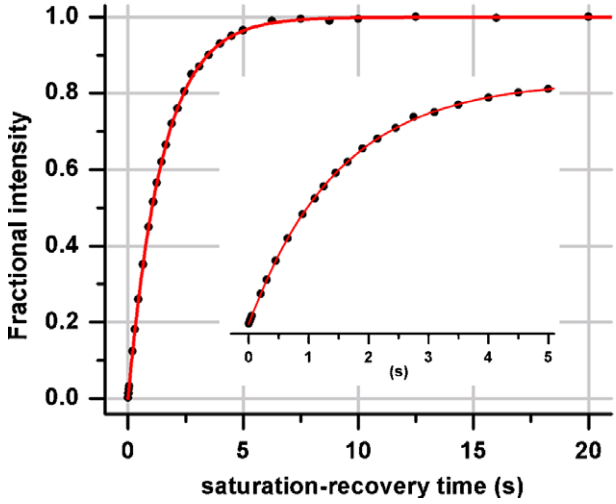

Fig. 12. ^{69}Ga magnetization recovery of the central transition with all transitions saturated initially, "CT(all-sat)," for a GaN film with the nuclear quadrupole coupling tensor symmetry axis oriented within 0.1° of the "magic-angle." The theoretical curve is an exponential fit with a time constant $\tau(^{69}\text{Ga}) = 1.50$ s, which by the procedure described in the text corresponds to values of $T_{1Q1} = T_{1Q2} \equiv T_{1Q}$ (^{69}Ga) = 1.54 s and $T_{1M}(^{69}\text{Ga}) = 51$ s.

This analysis suggested that the magic-angle orientation might be the most practically useful one for readily separating the magnetic and quadrupolar contributions to relaxation in GaN film samples, by measuring both ^{69}Ga and ^{71}Ga (all-sat) recovery curves. This idea is suggested by several considerations: (1) any experimental difficulties associated with providing the multiple irradiation frequencies needed for saturating all the transitions at other orientations, or with achieving good selectivity when saturating individual transitions, are removed; (2) rather than relying upon more complicated fitting procedures as has been done above to measure unequal T_{1Q1} and T_{1Q2} values and obtain T_{1M}, one can assume $T_{1Q1} = T_{1Q2}$ (as determined from the above experiments near the magic-angle and the experiment to be detailed below), with the result that the single-exponential recovery observed is due simply to two additive rate processes, the quadrupolar and the magnetic one, characterized by two time constants; (3) although one could assume that the quadrupolar time constant for the magic-angle orientation is known and invariant in all samples at a given temperature, and thereby obtain the two time constants from a single ^{71}Ga saturation-recovery curve, obtaining the ^{69}Ga saturation-recovery curve as well will provide a useful cross-check.

The use of ^{69}Ga results as a cross-check was carried out by aligning the GaN film exactly at the magic-angle (within an estimated 0.1°), as indicated by the collapse of the ST doublet to what appears to be a single peak in both the ^{71}Ga and the ^{69}Ga spectra (Figs. 9B and C, respectively). Both spectra reveal second-order effects upon the peak positions [8]: the CT position is shifted by $-\nu_Q^2/(4\nu_L)$, where the quadrupolar frequency ν_Q equals 860.2 kHz for ^{71}Ga and 1.365 MHz for ^{69}Ga, and the corresponding

Larmor frequencies ν_L are 152.58 and 120.08 MHz. The corresponding calculated second-order frequency shifts for the CT are −1.2 and −3.9 kHz. The (overlapping) ST position is shifted by $+\nu_Q^2/(3\nu_L)$, yielding calculated second-order frequency shifts for the ST of +1.6 kHz (^{71}Ga) and +5.2 kHz (^{69}Ga). The separation between ST and CT positions at the magic-angle should therefore be 2.8 kHz (^{71}Ga) and 9.1 kHz (^{69}Ga), which appears reasonably close to what is seen in Figs. 9B and C. The HHLW of the CT of ^{69}Ga is 3310 Hz, somewhat less than the value of 5040 Hz for ^{71}Ga; both CT peaks are sharper than the ST peaks, which are broadened by a distribution of NQCC values.

For this magic-angle orientation, the ^{71}Ga CT(all-sat) signal recovered with a single-exponential time constant $\tau(^{71}\text{Ga})$ of 3.47 s (data not shown), whereas the ^{69}Ga CT(all-sat) data fit very well to a single-exponential recovery time $\tau(^{69}\text{Ga})$ of 1.50 s, as seen in Fig. 13. (The ST recovery time could not be reliably determined, most likely because of the presence of an overlapping CT signal from a smaller higher-frequency Knight-shifted component; arbitrarily measuring the intensity of the left side of the ST at 200 ppm from the CT yielded a single-exponential time constant $\tau(^{69}\text{Ga})$ of 1.63 s, suggesting that the ST recovery time is close to that of the CT). The ratio of the ^{71}Ga to ^{69}Ga T_1 values for the CT at the magic-angle is 2.315, which is smaller than the ratio of the quadrupole moments squared (2.53) expected if the relaxation were entirely quadrupolar in origin.

We can attempt to quantitate the contribution from magnetic relaxation in two ways, one more complicated and one much simpler. The more complicated method follows the previously described strategy, and is to make the estimate $T_{1Q1}(^{69}\text{Ga}) = 1.63$ s from the ST results just mentioned, and then to fit the experimental results to Eq. (7) to obtain $T_{1Q2}(^{69}\text{Ga}) = 1.56$ s. A ^{69}Ga T_{1M} value of 73 s is then assumed, based upon scaling of the previously fit starting ^{71}Ga T_{1M} value of 45 s by the square of the magnetogyric ratios. The three ^{69}Ga relaxation time constants are then used in the analytical expressions [20] to obtain eigenrates and eigencoefficients, and then fit with the scaling factor (which turned out to be nearly equal for the CT and ST curves). Using the average scaling factor then resulted in the final values $T_{1Q1} = 1.66$ s, $T_{1Q2} = 1.59$ s, and $T_{1M} = 75$ s, which produces a theoretical recovery curve whose quality of the fit was nearly identical to that obtained with the single-exponential time constant, reflecting the near-equality of T_{1Q1} and T_{1Q2}. However, this involved procedure yields a ratio of the average of T_{1Q1} and T_{1Q2} for ^{71}Ga/^{69}Ga of $(3.75 + 3.79)/(1.66 + 1.59) = 2.32$, which is significantly less than the theoretical ratio of 2.53 mandated from the squared ratio of quadrupole moments. Thus, this complicated procedure, using the previously determined starting ^{71}Ga T_{1M} value (whose size relative to $T_{1Q1,2}$ is thus fixed), appears to have somewhat overestimated the magnitude of $T_{1M}(^{69}\text{Ga})$. The simpler (and more self-consistent) procedure described below uses the theoretically mandated ratio of 2.53 to obtain a somewhat smaller value for $T_{1M}(^{69}\text{Ga})$.

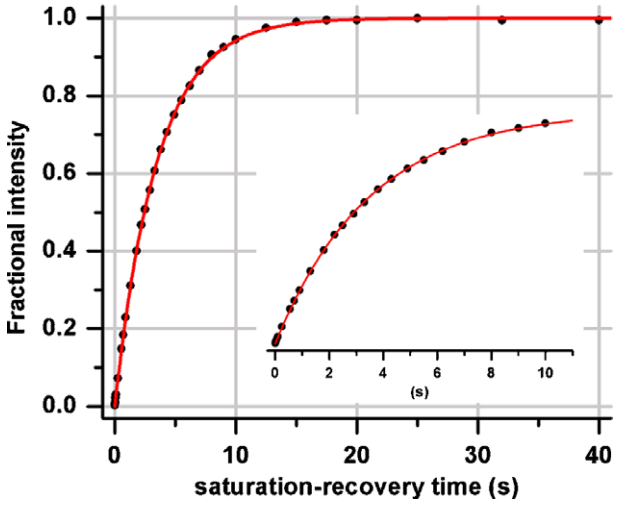

Fig. 13. ^{71}Ga MAS-NMR magnetization recovery of the central transition with all transitions saturated initially, "CT(all-sat)," for a polycrystalline GaN sample at 304 K. The theoretical curve is for a single-exponential fit with time constant $\tau(^{71}\text{Ga}) = 3.51$ s. See text for details.

The simpler procedure, which should be most useful for assessing the presence of n-type dopants in GaN films based upon their contribution to magnetic relaxation, is to assume $T_{1Q1} = T_{1Q2}$ *exactly*, and then to ask what fraction of the overall relaxation rate must be due to magnetic relaxation to produce the observed ^{71}Ga/^{69}Ga ratio of single-exponential rate constants.

The most convenient way to solve this latter problem is to note that when $T_{1Q1} = T_{1Q2} \equiv T_{1Q}$, the analytical expressions give a single eigenrate that we can call $1/\tau$ that is the sum of the quadrupolar and magnetic eigenrates $1/T_{1Q}$ and $1/T_{1M}$, respectively,

$$\frac{1}{\tau(^{69}\text{Ga})} = \frac{1}{T_{1Q}(^{69}\text{Ga})} + \frac{1}{T_{1M}(^{69}\text{Ga})}, \tag{9}$$

with an equivalent expression for ^{71}Ga as well. Since $T_{1Q}(^{71}\text{Ga}) = 2.5258\ T_{1Q}(^{69}\text{Ga})$ and $T_{1M}(^{71}\text{Ga}) = 0.6194\ T_{1M}(^{69}\text{Ga})$, as calculated from the squared ratios of the quadrupole moments and Larmor frequencies, respectively, we basically have two equations in two unknowns. Using the measured values of $\tau(^{69}\text{Ga}) = 1.50$ s and $\tau(^{71}\text{Ga}) = 3.47$ s yields the solutions $T_{1Q}(^{69}\text{Ga}) = 1.54$ s and $T_{1M}(^{69}\text{Ga}) = 51$ s, with the other isotope having the values $T_{1Q}(^{71}\text{Ga}) = 3.90$ s and $T_{1M}(^{71}\text{Ga}) = 31$ s (these values are listed in Table 2). While the $T_{1M}(^{71}\text{Ga})$ value obtained by this simple procedure is somewhat lower than the 46–49 s range obtained from the earlier analyses above, for at least the CT results near the magic-angle the fit using these values is also very good (a single-exponential $\tau(^{71}\text{Ga}) = 3.47$ s). For the other orientations, where $T_{1Q1} \neq T_{1Q2}$, attempts to test the fit using $T_{1M}(^{71}\text{Ga}) = 31$ s would be more involved, and were not carried out because the resultant changes in relaxation parameters and theoret-

ical curves would be expected to be minor. It is likely that the simple procedure proposed here, involving comparisons of ^{71}Ga and ^{69}Ga CT(all-sat) saturation-recovery curves of films oriented at the magic-angle, will give the most reliable comparisons between different film samples. Note that the magnetic contribution to the overall relaxation rate thus determined is only 11% for ^{71}Ga, and an even smaller 3% for ^{69}Ga.

4.2. MAS-NMR of powder sample

4.2.1. ^{71}Ga MAS-NMR

Fig. 13 shows the ^{71}Ga MAS-NMR saturation-recovery behavior for the polycrystalline GaN sample central transition with all transitions saturated initially by the incommensurate train of 90° pulses, "CT(all-sat)." The data fit very closely to a single-exponential recovery with time constant 3.51 s. Since the results below indicate that the relaxation is largely via the quadrupolar mechanism, we can assume the approximate T^3 temperature dependence of the quadrupolar relaxation rate observed by Corti et al. [14] to predict a time-constant of 3.76 s at the 297 K temperature of the film experiments. This is fortuitously close to the $T_{1Q1,2}$ average value of 3.77 s measured for the film with the tensor symmetry axis oriented at the magic-angle, and is also close to the perpendicular tensor symmetry axis film values of $T_{1Q1} = 3.85$ s and $T_{1Q2} = 3.42$ s (and somewhat less so to the parallel tensor symmetry axis film values of $T_{1Q1} = 4.54$ s and $T_{1Q2} = 3.44$ s).

A more fundamental comparison between the MAS-NMR and film results, for the situation in which the quadrupolar mechanism dominates, would entail: (1) calculating for the former the recovery curve for each family of crystallites having a specific cone angle with respect to the rotor axis; (2) summing up the properly weighted recovery curves for each cone angle. Each recovery curve would be obtained from Eq. (7) using the T_{1Q1} and T_{1Q2} values corresponding to an *average* over the rotor cycle, and thus would require explicit knowledge of these values at all tensor symmetry axis orientations with respect to the field. In general, the *difference* between the averaged T_{1Q1} and T_{1Q2} values would tend to be smaller than the difference between individual extremes, and would thus reduce the likelihood of being able to observe overshoots and undershoots such as depicted in Fig. 2.

Thus, reasonable semi-quantitative agreement between the ^{71}Ga MAS-NMR result and ^{71}Ga results from film experiments seems to hold, although accurate explicit comparison is not possible. When T_{1Q1} does not differ greatly from T_{1Q2}, as is true here, it seems likely that the CT(all-sat) experiment will exhibit single-exponential recovery. The general possibility exists of using a CT(sel-sat) experiment to tell whether $T_{1Q1} = T_{1Q2}$ in those cases where the quadrupolar mechanism dominates, since only then will the single-exponential time constant obtained according to Eq. (8) be identical to that obtained for the CT(all-sat) experiment according to Eq. (7). It is not clear how unequal the constants would have to be before measurable effects (taking into account the averaging of time constants over a rotor cycle discussed above) could be observed. Furthermore, achieving selective saturation of the CT is difficult: 90° pulses that are short compared to the rotor period will tend to excite some ST as well, and weaker 90° pulses will not be short compared to the rotor period (except at slow spinning speeds) and will thus also affect ST. One possible solution would be to rely on hyperbolic secant ST excitation pulses centered at some distance from the CT to achieve inversion of all ST without affecting the CT, as demonstrated recently [25]. The initial conditions for complete ST inversion of $N(0) = [-2, +3, -2]$ would lead to a CT signal decreasing from its 3-fold population-transfer enhanced value at $t = 0$ to its equilibrium value as $M_0[1 + 2\exp(-2W1t) + \exp(-2W2t)]$. Comparison with the CT(all-sat) recovery behavior would reveal any significant differences between $W1$ and $W2$ (and T_{1Q1} and T_{1Q2}). The possibility of interference from rotational resonance effects as previously noted [12,13] would have to be considered, and eliminated by spinning slightly away from the magic-angle if possible.

4.2.2. ^{69}Ga MAS-NMR

The ^{69}Ga "CT(all-sat)" saturation-recovery behavior of the polycrystalline GaN sample is shown in Fig. 14. Note that because the second-order quadrupolar broadening of the MAS spectrum is greater for ^{69}Ga vis-à-vis ^{71}Ga, the weak broader peak seen in the inset spectrum arising from the inhomogeneous distribution of Knight shifts [17]

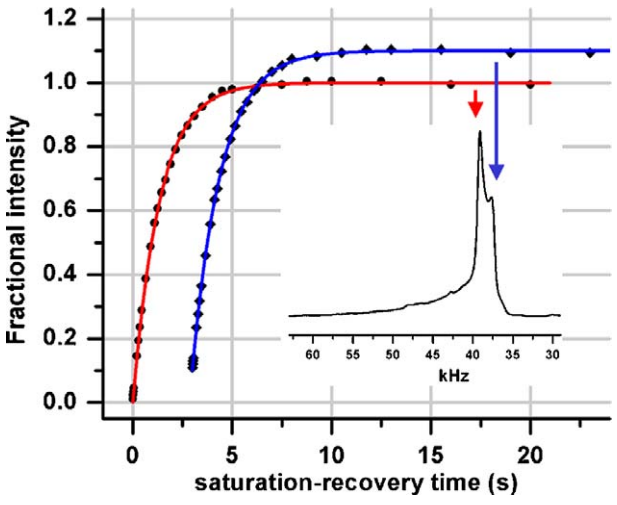

Fig. 14. ^{69}Ga MAS-NMR magnetization recovery of the central transition with all transitions saturated initially, "CT(all-sat)," for a polycrystalline GaN sample at 304 K. The inset shows the spectrum (obtained using an exponential apodization of 100 Hz linebroadening), which has the left and right singularities of a second-order broadened quadrupolar pattern, and arrows to the corresponding saturation-recovery curves (that for the right peak has been offset by $x = 3$ s and $y = 0.1$ for clarity). (The higher-frequency weak broad peak corresponds to portions of the sample that exhibit Knight shifts; the x-axis origin is arbitrary). The corresponding single-exponential time constants for the fits depicted are 1.35 and 1.47 s. See text for details.

becomes more noticeable (both ^{69}Ga and ^{71}Ga data were acquired using a rotor-synchronized Hahn spin echo that reveal this broader feature). The slight difference in single-exponential time constants obtained for the leftmost and rightmost singularities in the second-order-broadened MAS powder pattern (at the positions expected [21] taking into account the ^{69}Ga NQCC [15]) could be due to a small contribution to the measured intensity of the leftmost peak from a more rapidly relaxing Knight shifted component, or possibly to the fact that different families of crystallite orientations having different rotation-averaged relaxation rates $W1$ and $W2$ contribute to the leftmost and rightmost singularities. Whatever the origin of the slight differences, the ratio of the ^{71}Ga to ^{69}Ga exponential time constants is 2.60 and 2.38 for left and right peaks, with an average ratio of 2.49. This can be compared to the theoretical ratio of 2.53 expected if the relaxation were solely due to the quadrupolar mechanism. The combined ^{71}Ga and ^{69}Ga MAS-NMR results show that for this sample the relaxation is indeed dominated by the quadrupolar mechanism, and agrees (semiquantitatively at least) with the rates measured for the film sample. Obtaining ^{69}Ga (and ^{71}Ga) MAS-NMR saturation-recovery spectra at higher magnetic field strengths would narrow the width of the CT and thus improve the ability to obtain an accurate ratio of relaxation rates that reflects any small contribution from the magnetic mechanism.

5. Conclusions

The experimental strategy described here offers a useful way to employ multifrequency pulsed NMR techniques to create initial conditions for populations of levels of an oriented $I = 3/2$ quadrupole-perturbed spin system corresponding either to complete saturation of all transitions or to selective saturation. The use of time-consuming weak CW saturation requiring several T_1 intervals can thereby be avoided. By observing magnetization recovery of both CT and ST peaks in complete saturation (''all-sat'') experiments and by observing the selectively saturated CT peak magnetization recovery (''sel-sat''), the three time constants T_{1Q1}, T_{1Q2}, and T_{1M} could be obtained from a detailed analysis. Although the former experiments involved doing two separate experiments, one experiment would suffice if the splitting is small enough and the probe/excitation bandwidth is sufficient such that both transitions can be observed simultaneously with reasonable signal:noise. The existence of a second isotope (in this case ^{69}Ga) having different proportions of quadrupolar and magnetic relaxation contributions provided a useful, but not essential, cross-check of the parameters obtained.

The situation that applied to the most extensively studied orientation (a perpendicular tensor symmetry axis) involved T_{1Q1} and T_{1Q2} values that are close but unequal. This closeness of values presents the greatest challenges to accurate analysis due to the similarities of the two eigenrates involved in the fit. The difficulty experienced in assigning error bars in this case would be mitigated for more dissimilar T_{1Q1} and T_{1Q2} values, such as seen for the more limited parallel tensor symmetry axis experiments. However, the emphasis here has been on presenting a useful experimental strategy applicable to other $I = 3/2$ spin systems as well. Extensions of this strategy to higher half-integer quadrupolar spins are possible, although the lack of analytical expressions for eigenrates/eigencoefficients means that numerical matrix solutions will be required.

One important point emphasized by these experiments is that rather slight inequalities between the single-quantum T_{1Q1} and double-quantum T_{1Q2} time constants for quadrupolar relaxation can lead to apparent single-exponential relaxation behavior with time constants that lack direct physical significance. Since such inequalities between T_{1Q1} and T_{1Q2} can be orientation dependent, as is the case here, the magnetization-recovery behavior observed in MAS-NMR experiments may also exhibit apparent single-exponential behavior with time constants that also lack direct physical significance, and that may be somewhat different from those obtained from a single crystal.

In the case of MAS-NMR of GaN, the magnitude of such effects has been adumbrated, and the most practically useful means for sorting out magnetic and quadrupolar mechanisms seems to be comparing CT(all-sat) data for ^{71}Ga and ^{69}Ga, preferably at higher magnetic fields. For GaN single-crystal (film) samples, the identical comparison at the magic-angle orientation should provide a robust and sensitive method for measuring the magnetic contributions to relaxation in GaN film samples. For samples having larger relative contributions from magnetic relaxation, ^{71}Ga results alone would suffice if one assumes the quadrupolar rate measured here at 297 K, or some limited temperature extrapolation as measured by Corti et al. [14].

Acknowledgments

Dr. Kent Thurber is gratefully acknowledged for valuable discussions on relaxation in quadrupolar systems. We thank an anonymous referee for suggesting the numerical approximation when Eq. (7) yields apparent single-exponential relaxation behavior. Support from ONR to the NRL core program and from the DARPA spintronics program is acknowledged.

References

[1] R.V. Pound, Nuclear electric quadrupole interactions in crystals, Phys. Rev. 79 (1950) 685–702.
[2] E.R. Andrew, D.P. Tunstall, Spin–lattice relaxation in imperfect cubic crystals and in non-cubic crystals, Proc. Phys. Soc. 78 (1961) 1–11.
[3] D.G. Hughes, Nuclear quadrupole spin–lattice relaxation in single crystals for $I = 3/2$, Proc. Phys. Soc. 87 (1966) 953–965.
[4] M.I. Gordon, M.J.R. Hoch, Quadrupolar spin–lattice relaxation in solids, J. Phys. C 11 (1978) 783–795.

[5] T.J. Rega, Separation of magnetic and quadrupolar relaxation rates from spin–lattice recovery laws at short times with illustration in a high-T_c superconductor, Phys. Condens. Matter 3 (1991) 1871–1876.
[6] A. Suter, M. Mali, J. Roos, D. Brinkmann, Separation of quadrupolar and magnetic contributions to spin–lattice relaxation in the case of a single isotope, J. Magn. Reson. 143 (2000) 266–273.
[7] J. Van Kranendonk, M.B. Walker, Theory of spin–lattice relaxation in anharmonic crystals, Can. J. Phys. 46 (1968) 2441–2461.
[8] A. Abragam, The Principles of Nuclear Magnetism, Oxford Univ. Press, Oxford, 1961 (1970 printing).
[9] D.G. Hughes, P.A. Spencer, Orientation dependence of the Na-23 nuclear-quadrupole spin–lattice relaxation in sodium nitrite, J. Phys. C: Solid State Phys. 15 (1982) 7417–7428.
[10] T. Kanashiro, T. Ohno, M. Satoh, Orientation dependence of the quadrupole relaxation in $NaNO_3$, Jpn. J. Appl. Phys. 22 (1983) L253–L254.
[11] E.R. Andrew, K.M. Swanson, B.R. Williams, Angular dependence of nuclear spin–lattice relaxation time for several alkali halide crystals, Proc. Phys. Soc. Lond. 77 (1961) 36–48.
[12] D.E. Woessner, H.K.C. Timken, The influence of MAS on spin–lattice relaxation curves and nuclear-spin excitation of half-integer spin quadrupolar nuclei in solids, J. Magn. Reson. 90 (1990) 411–419.
[13] H.-T. Kwak, P. Srinivasan, J. Quine, D. Massiot, Z. Gan, Satellite transition rotational resonance of homonuclear quadrupolar spins: magic-angle effect on spin-echo decay and inversion recovery, Chem. Phys. Lett. 376 (2003) 75–82.
[14] M. Corti, A. Gabetta, M. Fanciulli, A. Svane, N.E. Christensen, ^{69,71}Ga NMR spectra and relaxation in wurtzite GaN, Phys. Rev. B 67 (2003), 064416-1 to -8.
[15] J.P. Yesinowski, ^{69,71}Ga and ^{14}N high-field NMR of gallium nitride films, Phys. Stat. Sol. (c) 2 (2005) 2399–2402.
[16] A.P. Purdy, J.P. Yesinowski, A.T. Hanbicki, Synthesis, solid-state NMR, and magnetic characterization of h-GaN containing magnetic ions, Phys. Stat. Sol. (c) 2 (2005) 2437–2440.
[17] J.P. Yesinowski, A.P. Purdy, H. Wu, M.G. Spencer, J. Hunting, F.J. DiSalvo, Abstract and oral presentation at Rocky Mountain Conference Solid-State NMR Symposium, Denver CO, July 2005, J. Amer. Chem. Soc. (submitted for publication).
[18] N. Bloembergen, Nuclear magnetic relaxation in semiconductors, Physica 20 (1954) 1130–1133.
[19] J.P. Yesinowski, A.P. Purdy, Defect dynamics observed by NMR of quadrupolar nuclei in gallium nitride, J. Am. Chem. Soc. 126 (2004) 9166–9167.
[20] A. Suter, M. Mali, J. Roos, D. Brinkmann, Mixed magnetic and quadrupolar relaxation in the presence of a dominant static Zeeman Hamiltonian, J. Phys.: Condens. Matter 10 (1998) 5977–5994.
[21] D. Freude, J. Haase, Quadrupole effects in solid-state nuclear magnetic resonance: in: NMR: Basic Principles and Progress, vol. 29, Springer, Berlin, 1993, pp. 1–90.
[22] A.F. McDowell, Magnetization-recovery curves for quadrupolar spins, J. Magn. Reson. A 113 (1995) 242–246.
[23] A. Bielecki, D.P. Burum, Temperature-dependence of ^{207}Pb MAS spectra of solid lead nitrate. An accurate, sensitive thermometer for variable-temperature MAS, J. Magn. Reson. A 116 (1995) 215–220.
[24] S.L. Segel, J.D. Stroud, Pseudoquadrupole interaction in gallium metal, J. Phys. F: Metal Phys. 5 (1975) 1986–1992.
[25] R. Siegel, T.T. Nakashima, R.E. Wasylishen, Signal enhancement of NMR spectra of half-integer quadrupolar nuclei in solids using hyperbolic secant pulses, Chem. Phys. Lett. 388 (2004) 441–445.